Bulgarian Chemical Communications, Volume 53, Issue 2 (pp. 249 - 255) 2021 DOI: 10.34049/bcc.53.2.5384

Preparation and thermal stability evaluation of GNP/CNT doped poly(lactic acid) and high-density polyethylene nanocomposites

V. F. Georgiev*

Institute of Catalysis, Bulgarian Academy of Sciences, Sofia 1113, Bulgaria
Institute of Mechanics, Bulgarian Academy of Sciences, Sofia 1113, Bulgaria

Received: February 11, 2021; Revised: March 16, 2021

Melt mixing was used to obtain two series of composite materials based on poly(lactic acid) (PLA) and high-density polyethylene, reinforced with 1.5% graphene nanoplatelets and multi-walled carbon nanotubes. Analysis methods such as infrared spectroscopy, wide-angle X-ray diffraction, and scanning electron microscopy were used to determine the materials' structural and chemical properties. Studies showed no intercalation or interaction of the polymer molecules with the fillers, approved by the absence of shift of the main diffraction peak of the fillers appearing at 26.3°, and the same wavenumbers of pure high-density polyethylene absorption bands compared to these of the composite materials. The differential scanning calorimetry showed that the addition of fillers did not affect the glass transition temperature and the melting temperature of PLA but had a slight effect on melt crystallization which increased by 7° for the 1.5% GNP/1.5% CNT/PLA sample. Thermal stability was improved for the 1.5% GNP/PLA material as the decomposition onset temperature increased by 2 ºC, determined by thermogravimetric analysis. High-density polyethylene-based composite materials with the presence of graphene nanoplatelets are characterized by a 2 °C increase in melting point and an 8 °C increase in the onset of decomposition temperature for the bifiller ones. It can be attributed to the high aspect ratio of GNPs that served as a barrier and then prevented the emission of gaseous molecules during thermal degradation.

Keywords: thermal stability, composite, graphene.

INTRODUCTION

The increased interest to polymer stability research has been discussed in a great number of papers [1-3]. High-density polyethylene (HDPE) and poly(lactic acid) (PLA) possess a combination of favorable physical properties, chemical resistance, and economic characteristics that make them incredibly versatile and suitable in various applications. Poly(lactic acid) is well known as a biodegradable polymeric material produced from agricultural resources that has recently found application in fused deposition modeling [4]. At the same time, HDPE has found widespread use in products designed for outdoor applications where degradation from sunlight and other weathering conditions becomes an essential factor. For the polymers successfully to withstand degradative oxidation accelerated by high processing and service temperatures, as well as outdoor weathering conditions, a stabilizer or combination of stabilizers must be incorporated. Due to the controlled combination of the components, new materials with distinct properties are obtained from the individual components [5]. The typical fillers used in polymeric composites are graphene [6, 7] graphene oxide [8-10], silica [11, 12], and carbon nanotubes (CNTs) [13, 14]. Carbon nanotubes and graphene exhibit unique and unusual electrical, mechanical and thermal properties making them attractive fillers for reinforcing polymers to form functional and structural composite materials with high performance. The effective enhancement of mechanical, electrical and thermal properties by adding CNTs and graphene nanoplatelets (GNPs) in the polymer composites has been approved [15-17]. The main factor that could control the composite's potential properties is the degree of dispersion, percolation threshold, and interfacial interactions. Better dispersion and stronger interfacial interaction of both 2D and 1D fillers in the matrix polymer resulted in higher values of thermal conductivity, due to stronger suppressing of phonon scattering [18]. Unfortunately, carbon nanofillers with large surfaces and proportions are usually poorly dispersed in organic solvents and polymers. Neat carbon nanotubes CNTs and GNPs tend to form bundles or agglomerates due to the strong van der Waals interaction between them, which leads to weak interphase interactions between nanotubes and polymer matrix. The dispersion of carbon fillers in solvents and polymers can be improved by mechanical mixing and chemical functionalization. The melt mixing process employs high temperature and intense shear forces to disperse nanofillers in the molten polymer using rotating screws of an extruder. Its simplicity and low cost make it a promising technique for producing polymer composites with improved properties.

* To whom all correspondence should be sent:
E-mail: vlado@ic.bas.bg

In this paper we report the effect of multiwalled carbon nanotubes and graphene nanoplatelets addition into poly(lactic acid) and high-density polyethylene on the resulting nanocomposites' thermal stability. Hot melt mixing was applied for fabrication of composites with filler content of 1.5%wt. denoted as 1.5% GNP/PLA, 1.5% CNT/PLA, 1.5% GNP/HDPE, 1.5% CNT/HDPE, 1.5% GNP/1.5% CNT/PLA and 1.5% GNP/1.5% CNT/HDPE.

MATERIALS AND METHODS

Materials

The poly(lactic) acid (PLA-3D850) with MFR 7–9 g/10 min (210 ◦C, 2.16 kg), peak melt temperature 165-180 ◦C, and glass transition temperature 60–65 ◦C was supplied by Nature Works, USA. Industrial GNPs and industrial grade OH-functionalized multiwall carbon nanotubes adopted as nanofillers were supplied from Times Nano, China. GNPs purity is 90% and true density is 2.2 g/cm^3, whereas CNT purity is 95%, true density is 2.1 g/cm^3 and its OH-content is 2.48%.

Preparation of Nanocomposites

Two series of nanocomposite materials based on PLA and HDPE with GNPs and CNTs content of 1%wt. were produced by melt mixing using the twin-screw extruder, COLLIN Teach-Line ZK25T, with a screw speed of 40 rpm for PLA composites and Thermo Scientific twin screw extruder at 100 rpm and temperatures of 170–180 °C. Before mixing with the fillers, the PLA pellets were ground and then used as a powder for 9% masterbatch preparation while the HDPE mixture was prepared by wrapping technique in a ball mill for two hours at a speed of 70 rpm. Then, the formulations with lower filler contents of 1.5 wt. % were prepared by diluting the respective masterbatches with neat PLA and HDPE through a second extrusion run.

Experimental Methods

Wide-angle X-ray diffraction (WAXD) was employed for characterization of the samples. The measurements were performed on a DX-1000 X-ray diffractometer (Dandong Fangyuan Instrument Co., Ltd., Dandong, Liaoning Province, China) employing copper line focus X-ray tube producing Kα radiation by a generator operating at 45 kV and 25 mA. The diffraction patterns were taken in the range from 5◦ to 70◦ at a 1◦/min rate. The specimens being analyzed were powders for the fillers, GNPs and MWCNTs and pellets for the nanocomposites. The data from WAXD were processed using MDI Jade software capable of analyzing the crystal structure of materials. The KBr technique was applied for recording the FT-IR spectra in the scanning range from 4000 to 400 cm^{-1} using a Nicolet 6700 spectrometer. The morphology and structures were visualized using scanning electron microscopy (SEM) on a Quanta 250 instrument (FEI Co. Ltd, USA).

DSC Q20 (TA Instruments), was used for the DSC measurements. The test sample with a weight of ~10 mg was placed in an aluminum pan and hermetically sealed in order to prevent gas emissions into the instrument or in the environment. Tests were performed in two cycles (one heating and one cooling scan). During the heating cycle, the temperature was raised from room temperature to 200 °C, with a ramp of 10 °C/min, and held for 1 min. Afterward, the temperature was lowered from 200 °C to 20 °C in order to register the DSC curve through the cooling cycle. Upon these conditions, the glass transition temperature (T_g), melt crystallization temperature (T_c) and melting peak temperature (T_m) were determined from the heating and cooling DSC curves. TGA Q50 (TA Instruments) was used for the thermo-gravimetric analysis (TGA) measurements. It was done to assess the composite thermal stability defined by the characteristic decomposition temperatures of the samples. The trials were performed in nitrogen atmosphere by heating a 10 mg specimen from room temperature to 600 °C in an aluminium pan, with a heating step of 10 °C/min.

RESULTS AND DISCUSSION

WAXD analysis was used to characterize the nanocomposites as it provided accurate information on the phase composition and crystallinity of the test materials. Fig. 1 shows pure graphene nanoplatelets characterized by a main reflection (002) peak at 2θ = 26.35°, sharper than that of the carbon nanotubes' peak at 2θ = 26° from the corresponding diffraction plane, indicating a more crystalline structure of GNPs. The shifting of the nanotubes diffraction peak (002) to lower degrees (2θ = 26°) means a larger interplanar spacing between the lattice fringes which could be assigned to higher functionalization of the CNTs in comparison to GNPs. By applying the Scherer equation, $L_{hkl} = k\,\lambda\,/(\beta_{hkl}\,cos\,\theta)$, where: β is the FWHM of the reflection (in radians) located at 2θ, with an appropriate value of the shape factor of k = 0.9, it was found that the GNPs powders have a stack thickness of about 18 nm. The addition of carbonaceous fillers does not increase the PLA's crystallinity for both series, which is evident from the comparison of the WAXD spectra of the pure polymer and those of the composite materials (Fig. 1). It is seen that there is no appearing of a sharp peak

in the composites' patterns containing 1.5% CNTs or GNPs at around 16.8 degrees [19], which would be due to crystal areas' formation, but only the wide halo characteristic of amorphous PLA with a steepest point at 2θ = 15.5° remains unchanged.

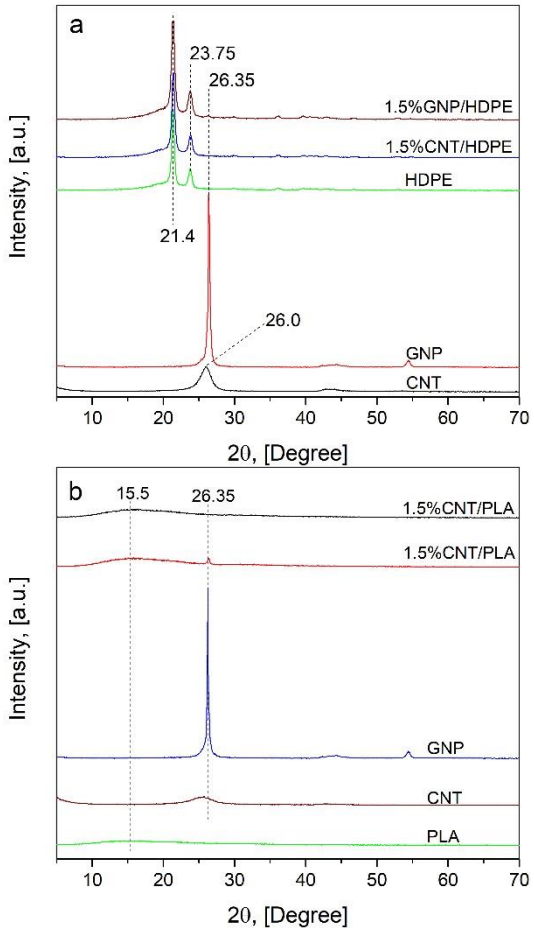

Fig. 1. X-ray diffraction spectra of (a) series of HDPE and (b) series of PLA.

This is attributed to the insufficient fillers nucleation effect to cause a significant increase in the crystallinity of the PLA. In the spectra of 1.5% CNT/PLA and 1.5% CNT/HDPE, no additional peaks were found due to filler presence in the mixed materials, probably because of its small particle size and homogeneous dispersion in the volume of the polymer. Characteristic of the composite materials spectra containing 1.5% GNP is the appearance of a peak at 26.35° which is attributed to pure GNPs. Since a shift of this peak was not observed, it can be concluded that no intercalation of polymer molecules occurred in the stacks of graphene particles.

SEM micrographs of 1.5% GNP/HDPE and 1.5% GNP/PLA are shown in Fig. 2. The images show that the filler particles are distributed in the polymer's volume with any spatial orientation for 1.5% GNP/HDPE. It was reported [20] that GNPs have intrinsic properties to orient predominantly in-plane that impedes the practical application, which was observed for 1.5% GNP/PLA. Such anisotropy mostly affects the thermal conductivity (the thermal conductivity of in-plane is much higher than that of through-plane) in GNP-based thermal composites.

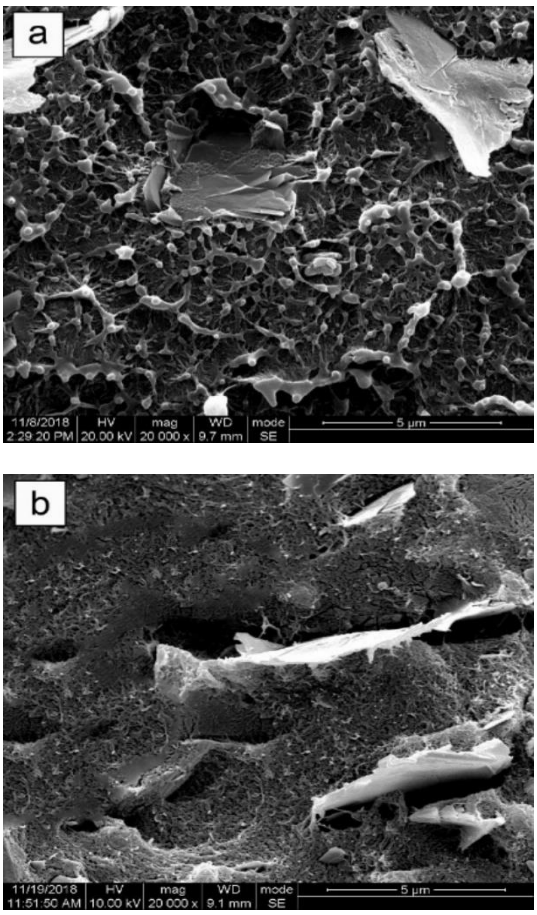

Fig. 2. SEM micrographs of (a) 1.5% GNP/HDPE and (b) 1.5% GNP/PLA samples.

To monitor the functionalization of GNPs and CNTs, FTIR analysis was conducted. Fig. 3 presents the FT-IR spectra in the scanning range from 4000 to 400 cm^{-1} for the tested samples of both series.

It is seen that characteristic bands appearing in the spectra of both fillers are at the same wavenumbers, which means that they possess the same functional groups. In the IR-spectra of GNP and CNT bands corresponding to stretching vibrations of the CH group at 2850 cm^{-1} and 2920 cm^{-1} are observed. The bands at 3436 cm^{-1}, 1630 cm^{-1}, 1110 cm^{-1} and 1052 cm^{-1} are due to stretching vibrations of the –OH, C=O and C–O adsorption groups, respectively. By comparing the spectra of the pure fillers and those of the composite materials, it is noticed that the peaks characteristic for the fillers are not present in the spectrum of the composite materials, probably due to their low concentration. Analysis of the IR spectra also shows no changes in the frequency of the vibration bands assigned to pure PLA or HDPE compared to the corresponding ones in the spectra of

the composite materials containing 1.5% filler. It follows that no new bonds are formed between the filler and the polymer, such as hydrogen bonding or strong van der Waals forces due to a direct interaction of a specified group and the adsorption site of the liquid matrix.

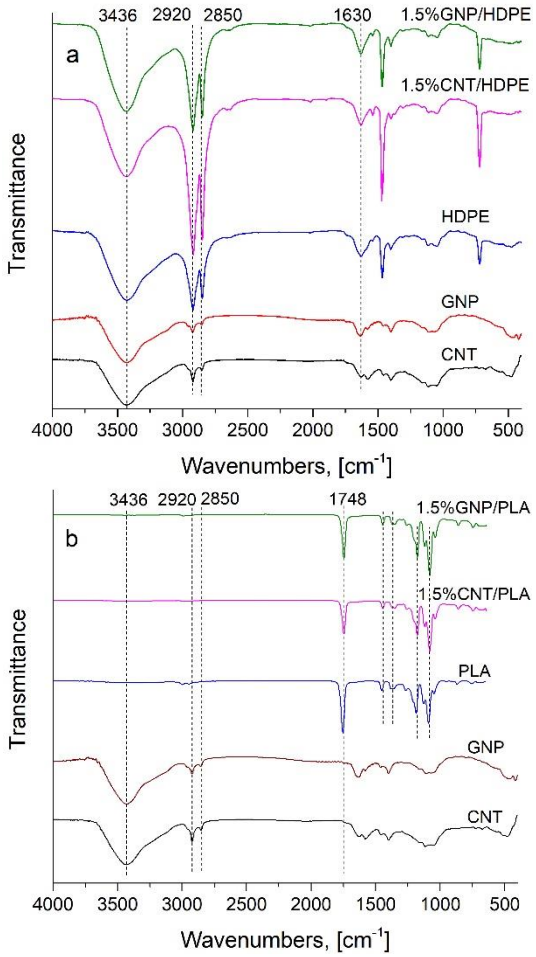

Fig. 3. IR spectra of (a) series of HDPE and (b) series of PLA.

Figures 4a and 4b present results from the DSC analysis of monofiller (GNP/PLA, CNT/PLA) and bifiller (GNP/CNT/PLA) nanocomposites containing 1.5 wt% carbon particles. The glass transition temperature for all nanocomposites is around 64-65°C. The transition region in which an amorphous glassy polymer changes from its glassy state into a rubber-like state is important because dramatic changes in the polymer's physical properties are observed during this transition. These changes are completely reversible as the transition from a glassy into a rubbery state. When considering the T_g of reinforced polymers, it should be had in mind that it depends mainly on the interaction of the polymer with the filler that impedes the relaxation [21]. The Tg increases, and *vice versa* if there is a repulsion between the filler and the polymer chain.

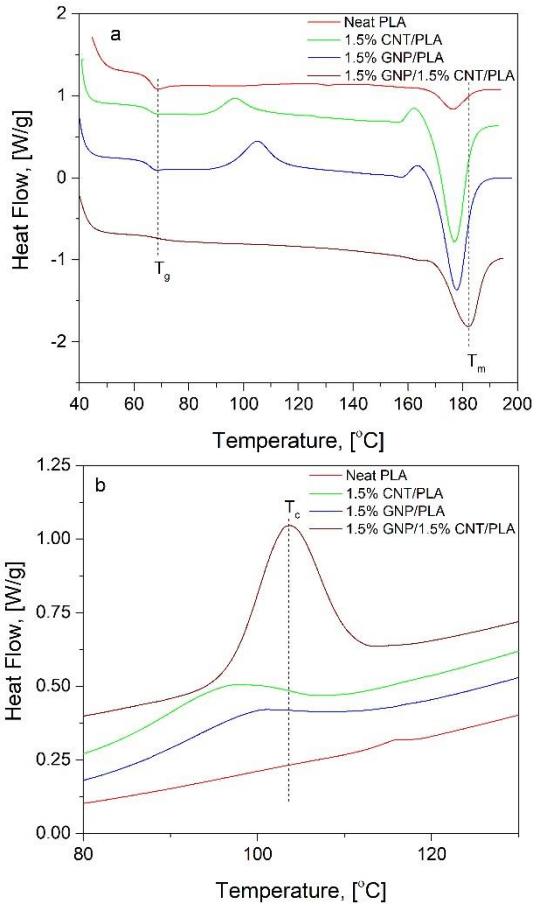

Fig. 4. DSC thermograms of (a) PLA, 1.5wt% GNP/PLA, 1.5wt% MWCNT/PLA and mixed composites during heating cycle and (b) during cooling cycle.

The similar Tg values of the samples (Table 1) imply either that the amount of nanofiller is insufficient to influence the composite Tg temperature or there is no strong interaction of attraction or repulsion between the carbon nanoparticles and the polymer.

Table 1. Thermal properties of samples after melting at 200° for pure PLA, monofiller (GNP/PLA, CNT/PLA) and bifiller (GNP/CNT/PLA) nanocomposites.

Samples	T_g [°C]	T_m [°C]	T_c [°C]
PLA	63.8	178.4	96.2
1.5% CNT/PLA	65.0	177.1	97.8
1.5% GNP/PLA	64.5	177.8	99.7
1.5%GNP/1.5%CNT/PLA	64.9	178.9	103.4

The melting temperatures for all tested PLA composite samples are in the range of 177-179 °C, and it can be concluded that the presence of nanofillers does not lead to a change compared to that of the pure PLA. Since the addition of fillers to the polymer does not increase the crystallinity of the

resulting materials, which is confirmed by XRD, in this case the melting temperature does not change significantly, because when considering semi-crystalline polymers, crystallinity directly affects the melting temperature. It can be seen from Fig. 4b that the melt crystallization of 1.5% GNP/CNT/PLA is higher by around 7°C compared to the pure PLA (Tc = 96.2°C). This observation is attributed to the synergic effect of GNPs and CNTs promoting the crystallization through heterogeneous nucleation during the cooling run.

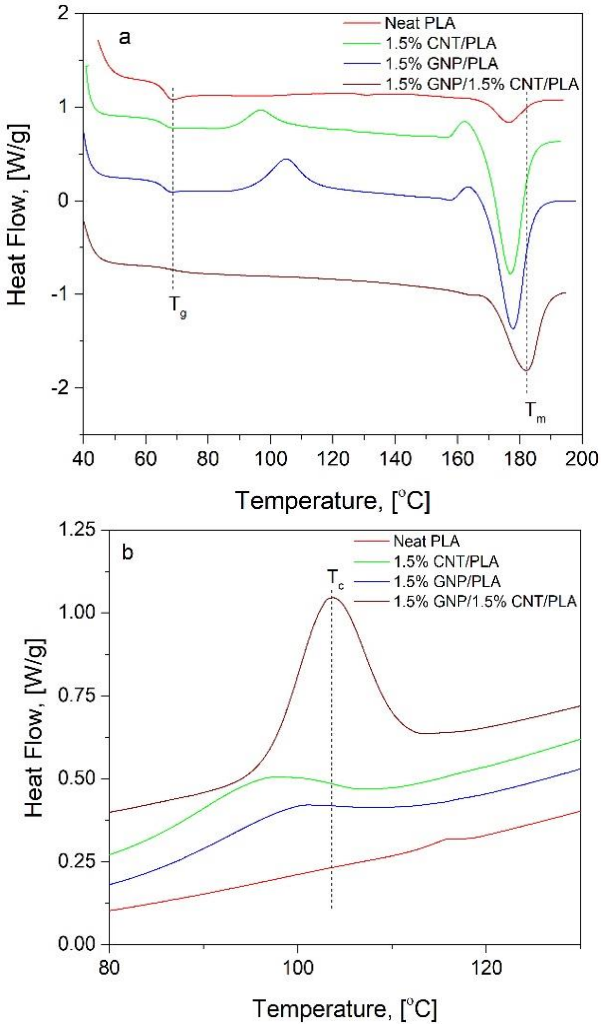

Fig. 4. DSC thermograms of (a) PLA, 1.5wt% GNP/PLA, 1.5wt% MWCNT/PLA and mixed composites during heating cycle and (b) during cooling cycle.

Figures 5a and 5b present DSC analysis results of pure HDPE and nanocomposites on its base containing 1.5wt% of carbon fillers. The melting temperature (T_m) of composite materials is by about 3 degrees higher than that of the pure polymer.

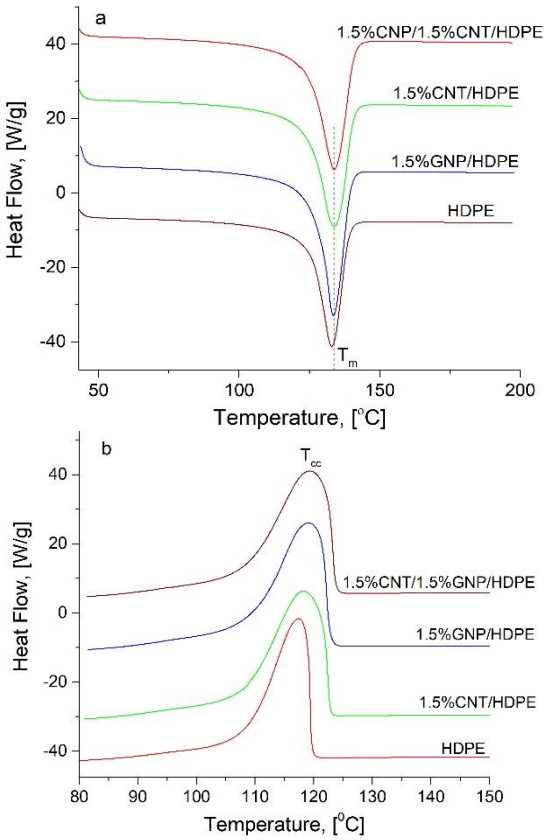

Fig. 5. DSC thermograms of (a) HDPE, 1.5wt% GNP/HDPE, 1.5wt% MWCNT/HDPE and mixed composites during heating cycle and (b) during cooling cycle of the same specimens.

The T_m of the pure HDPE is 132.1 °C, while those of the composites 1.5% GNP/HDPE and 1.5% GNP/1.5% CNT/HDPE are around 134 °C (Table 2). The melt crystallization slightly increases with adding fillers as for pure polymer, Tc = 116°C, while for the composites, it reaches 119.1°C for 1.5% GNP/HDPE. The shift of the crystallization and melting peaks to higher temperatures is due to an increased crystal size distribution due to nucleation.

Table 2. DSC thermal properties of samples after melting at 200° for monofiller (GNP/HDPE, CNT/HDPE) and bifiller (GNP/CNT/HDPE) nanocomposites.

Samples	T_g [°C]	T_m [°C]	T_c [°C]
HDPE	n/a	132.1	116.0
1.5% CNT/HDPE	n/a	133.7	118.2
1.5% GNP/HDPE	n/a	134.1	119.1
1.5%GNP/1.5%CNT/HDPE	n/a	133.7	118.2

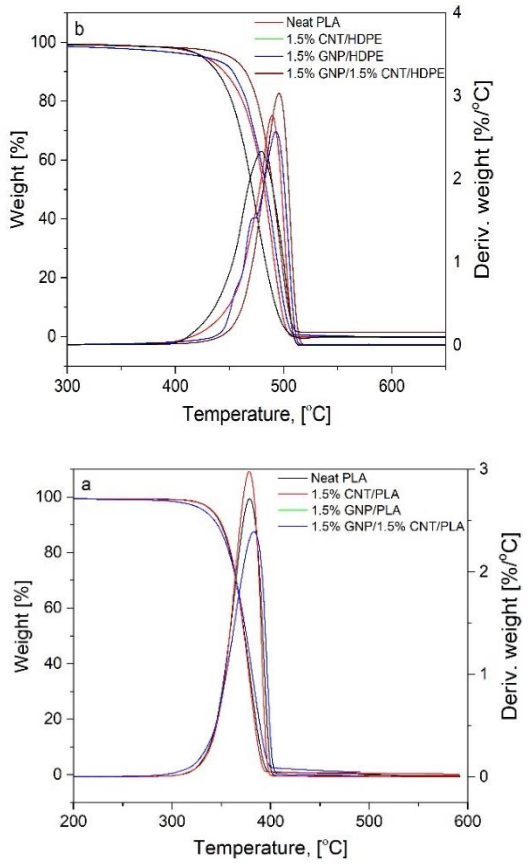

Fig. 6. TGA curves of (a) pure PLA, mono- and bifiller GNP/CNT composites and (b) pure HDPE, 1.5wt% GNP/HDPE, 1.5wt% MWCNT/HDPE, 1.5% GNP/1.5% CNT/HDPE

Thermogravimetry (TG), was applied to monitor mass loss as a function of the temperature at a constant heating rate in order to get a quick impression of the composite materials' thermal stability. The results are presented in Figure 6 and Table 3. Variation in weight percentage of the samples with respect to the temperature was observed. The values summarized in Table 3 represent the TGA characteristics of monofiller and bifiller composites. The thermal degradation process of PLA begins at 310.8 °C (onset temperature according to ASTM E2550) due to intra-molecular trans-esterification [22]. Afterward, a major degradation proceeds wherein the polymer chain breaks at a high rate in the range from 330 to 395 °C. Concerning the composites, the results apparently disclose that the composite 1.5% GNP/PLA improves the thermal stability of PLA with 2 °C as a result whereof T_{onset} raises to 312.9 °C. A possible explanation for this delayed breakdown can be the assumption that graphene nanoplatelets impede the diffusion of the gaseous low-mass degradation products from the bulk to its surface creating a labyrinth effect [23]. Another important point characterizing the thermal behavior is the pattern of the TGA curve depicting the overall mechanism of degradation. From Fig. 6a is visible that the samples undergo one-step destruction caused by C-C cleavage. Maximum improvement of the thermal degradation stability regarding the highest decomposition rate was observed for bifiller composites. Combining both fillers (GNPs and CNTs) the peak of polymer degradation T_p shifts to the higher temperatures with almost 9°C, due to the better spatial structure in the composite volume suppressing the heat distribution.

From the weight loss plots of HDPE's series (Fig. 6b) is seen that the onset of thermal degradation (T_{onset}) for neat HDPE is 354 °C. T_{onset} increases by about 4 K on the addition of 1.5%GNP and by 8 K on 1.5% addition for both fillers. The composite material containing 1.5% CNT shows the lowest T_{onset}, which is by about 40 K lower than that of the pure polymer. This behavior would suggest that at low CNT loadings, the CNTs accelerate the thermal degradation of HDPE and may be associated with the high thermal conductivity of CNTs and more effective dissipation of thermal energy. It has been proposed that CNTs create a 'barrier effect' by preventing the release of volatiles and decomposed products from the composite material, resulting in the retardation of the thermal decomposition of the composites, but a critical concentration of CNTs is required to enhance the thermal stability of HDPE.

Table 3. Values of T_{onset}, $T_{50\%}$, T_p, for PLA and HDPE monofiller (GNP, CNT) and bifiller (GNP/CNT) composites.

Samples	T_{onset} [°C]	$T_{50\%}$ [°C]	Peak of polymer degradation T_p [°C]
PLA	310.8	381.0	378.6
1.5%CNT/PLA	288.2	375.4	383.1
1.5% GNP/PLA	312.9	373.2	378.2
1.5%GNP/1.5%CNT/PLA	311.1	379.1	386.9
HDPE	354.2	482.1	489.4
1.5%CNT/HDPE	309.5	484.2	479.6
1.5% GNP/HDPE	357.8	471.6	492.7
1.5%GNP/1.5%CNT/HDPE	362.6	490.1	495.7

The thermal stability of HDPE is better demonstrated by examining the derivative weight as a function of temperature. Here, the peak maximum (T_p) is decreased for 1.5%CNT content, suggesting that the onset of thermal degradation of HDPE is shifted to lower temperatures. The unpredictability of HDPE/CNT composites' thermal stability implies that this property is controlled by a combination of factors, including CNT dispersion and distribution, the properties of the thermal conductivity of CNTs, polymer–CNT interactions and polymer crystallinity. The thermal stability increased for the GNP-added composites, attributed to the high aspect ratio of GNP that served as a barrier and then prevented the emission of gaseous molecules during the thermal degradation. Besides, the radical scavenging function of GNP could inhibit the degradation process of the polymer.

CONCLUSION

The thermal properties of two series of mono- and bifiller composite materials based on PLA and HDPE with 1.5% carbonaceous fillers content were evaluated. Test results showed that fillers addition to the base polymer had a small effect on the investigated materials' thermal properties. Glass transition temperature (T_g) for the PLA series was not affected by the presence of fillers, which is explained by the absence of interaction between the individual components of the composite. The same applies to the melting temperature (T_m), which for all samples is in the range of 178-179 °C, but melt crystallization of 1.5%GNP%CNT/PLA is higher by around 7 °C compared to the pure PLA (T_c = 96.2 °C). The decomposition's onset temperature (T_{onset}) obtained from the TGA analysis was increased by 2 °C for the 1.5% GNP/PLA sample. As for the HDPE series, the melting temperature of the composite materials is by about 3 °C higher than that of pure polymer and T_{onset} increased by about 4 °C on the addition of 1.5%GNP and by 8 °C on 1.5% addition of both GNP and CNT fillers.

Acknowledgement: *The author gratefully acknowledges financial support from Project BG05M2OP001-1.001-0008 National center on mechatronics and clean technologies; the H2020-FET-Graphene Flagship-881603-Graphene Core 3; and the Bulgarian National Science Fund contract KP-06-COST-11 (to CA19118).*

REFERENCES

1. A. Hassan, A. Akbari, N. Hing, Ch. T. Ratnam, *Polym Plast Technol Eng*, **51**(5), 473 (2012).
2. D. W. Sauter, M. Taoufik, Ch. Boisson, *Polymers*, **9**, 185 (2017).
3. J. Yu, L. Sun, Ch. Ma, Yu Qiao, H. Yao, *Waste Management*, **48**, 300 (2016).
4. A. Mushtaq, A. Israr, M. Fahad, J. Ahmed, *Bulgarian Chemical Communications*, **52**(1), 29 (2020).
5. I. Plesa, P. V. Notingher, S. Schlögl, Ch. Sumereder, M. Muhr, *Polymers*, **8**, 173 (2013).
6. S. Chatterjee, F. Nafezarefi, N. H. Tai, F. A. Nüesch, B. T. T. Chu, *Carbon*, **50**(15), 5380 (2012).
7. X. Huang, C. Zhi, P. Jiang, *J. Phys. Chem. C*, **116(**44), 23812 (2012).
8. N. Jha, P. Ramesh, E. Bekyarova, M.E. Itkis, R. Haddon, *Adv. Energy Mater*., **2**(4), 438 (2012).
9. F. Mohandes, M. Salavati-Niasari, *RSC Adv.*, **4**, 25993 (2014).
10. F. Mohandes, M. Salavati-Niasari, *J. Nano Res*., **16**, 2604 (2014).
11. J. W. Brinke, S. C. Debnath, L. A. Reuvekamp, J. W. Noordermeer, *Compos. Sci. Technol.*, **63**(8), 1165 (2003).
12. W. Kaewsakul, K. Sahakaro, W. K. Dierkes, J. W. Noordermeer, *Rubber Chem. Technol.*, **85**(2), 277 (2012).
13. 12. H.D. Bao, Z.X. Guo, J. Yu, *Polymer*, **49**(17), 3826 (2008).
14. T. Fukushima, A. Kosaka, Y. Yamamoto, T. Aimiya, S. Notazawa, T. Takigawa, T. Inabe, T. Aida, *Adv. Sci.*, **2**(4), 554 (2006).
15. R. Kotsilkova, I. Petrova-Doycheva, D. Menseidov, E. Ivanov, A. Paddubskaya, P. Kuzhir, *Compos. Sci. Technol.*, **181**(8), 107712 (2019).
16. G. Spinelli, P. Lamberti, V. Tucci, R. Kotsilkova, E. Ivanov, D. Menseidov, C. Naddeo, V. Romano, L. Guadagno, R. Adami, D. Meisak, D. Bychanok, P. Kuzhir, *Materials*, **12**(15), 2369 (2019).
17. E. Ivanov, R. Kotsilkova, H. Xia, Y. Chen, R. K. Donato, K. Donato, A. P. Godoy, R. Di Maio, C. Silvestre, S .Cimmino, V. Angelov, *Applied Sciences*, **9**(6), 1209 (2019).
18. R. Kotsilkova, E. Ivanov, V. Georgiev, R. Ivanova, D. Menseidov, T. Batakliev, V. Angelov, H. Xia, Y. Chen, D. Bychanok, P. Kuzhir, R. Di Maio, C. Silvestre, S. Cimmino, *Polymers*, **12**(6), 1208 (2020).
19. E. Teixeira, A. Campos J.M. Marconcini, T.J. Bondancia, D. Wood, A. Klamczynski, L. Mattoso, G. Glenn, *RSC Advances*, **4,** 6616(2014).
20. Q. Li, X. Tian, M. Wu, Y. Li, J. Pan, B. Zhang, Y. Duan, Sh. Wang, Y. Li, *J. Appl. Polym. Sci*., **138**, e49781 (2020).
21. K. Hagita, H. Morita, *Polymer*, **178**, 121615 (2019).
22. R. B. Valapa, G. Pugazhenthi, V. Katiyar, *RSC Adv.*, **5,** 28410 (2015).
23. I. Armentano, E. Fortunatu, N. Burgos, F. Dominici, F. Luzi, S. Fiori, A. Jimenez, K. Yoon, J. Ahn, S. Kang, J. M. Kenny, *Express Polymer Letters*, **9**(7), 583 (2015).